ISSN 1054-660X, Laser Physics, 2011, Vol. 21, No. 9, pp. 1638–1644.

Variable Gain-Flattened L-band Erbium-Doped Fiber Amplifier[1]

M. H. Abu Bakar[a], S. J. Sheih[b], F. R. Mahamd Adikan[c], and M. A. Mahdi[a, *]

[a] *Wireless and Photonics Networks Research Center, Faculty of Engineering, Universiti, Putra Malaysia, 43400 UPM Serdang, Selangor, Malaysia*

[b] *Taiwan International Securities Group, 33F, No. 97, Tun-Hwa S. Rd., Sec. 2, Taipei 106, Taiwan*

[c] *Department of Electrical Engineering, Faculty of Engineering, Universiti Malaya, 50603 Kuala Lumpur, Malaysia*

*e-mail: mdadzir@eng.upm.edu.my; adzir@ieee.org

Received February 26, 2011; in final form, March 18, 2011; published online August 3, 2011

Abstract—This is a study on the design of variable gain-flattened erbium-doped fiber amplifier operating in L-band transmission window. Four amplifiers divided into five stages became the basis of the design with distributed pumping configuration. A dispersion compensating module was incorporated into the architecture as a way to combat dispersion. The amplifier was able to generate variable gain from 15 up to 30 dB under different input signal powers with a maximum output power of 23 dBm. Excellent gain flatness averaging around 0.8 dB was accomplished while four-wave mixing effect was significantly reduced.

DOI: 10.1134/S1054660X11170014

INTRODUCTION

The introduction of erbium as a core element in rare-earth-doped fibers has sparked numerous studies in fiber lasers [1–3] and optical amplifiers. Erbium-doped fiber amplifier (EDFA) has been at the forefront in optical amplification field due to its ability to produce substantial gain under low pumping power plus its versatility in providing amplification in S-band [4, 5], C-band, and L-band [6]. Its wideband amplification spectrum makes it suitable for the employment of wavelength-division multiplexed (WDM) transmission. The use of WDM transmission system entails the propagation of multiple signals at small spacing which makes the system susceptible to nonlinearities such as four-wave mixing (FWM). This problem is further compounded in the C-band region in systems utilizing dispersion-shifted fiber (DSF) which has a zero-dispersion wavelength located at 1550 nm [7].

The introduction of L-band transmission window which is located further away from the zero-dispersion wavelength of DSF aids in minimizing the effect of FWM [7]. The L-band contribution to the betterment of WDM transmission can also be assessed from the additional bandwidth provided by the transmission window plus its low ripple spectrum which allows for a less stringent specification of gain-equalization filter (GEF) needed to produce level gain [8]. However, location of the L-band window at the lower tail end of erbium emission spectrum impedes the generation of high gain coefficient therefore dictating the use of gain enhancement techniques in L-band EDFA [9].

Due to geographical and infrastructural factors, transmission spans in an optical communication system are not necessarily of similar length. The different fiber length in transmission spans exposes transmission signals to different quantity of losses thus emphasizing the need for variable gain amplifiers that can cater to varying amount of input signals. With this capability, the EDFA will be capable of sustaining constant output power for dynamically changing input channels [10–12]. In addition, flat gain spectrum is also a necessity for multi channels transmission in order to maintain uniform gain as channels are added or dropped [13, 14]. This function is made simpler owing to the natural flat gain spectrum of erbium in L-band region but the employment of GEF is still required to handle gain variation in high operating gain regime [15].

It is also essential in WDM transmission to have a dispersion compensation scheme. The innovation of optical amplifier allows the deployment of longer transmission span, subjecting transmission signals to higher accumulated dispersion. The addition of dispersion compensating module (DCM) is considered as an effective way of countering dispersion but at the expense of additional losses in the transmission. A research was performed on a technique to minimize DCM loss by utilizing it as a discrete Raman amplifier which is a less attractive approach due to the need for high pump power [16]. The assimilation of EDFA and DCM seems to be a better choice in minimizing the additional loss of DCM. Nevertheless, the requirements of tight signal conditioning lead to strict management of fiber dispersion, gain uniformity, optical signal-to-noise ratio (OSNR) and gain dynamic. These added features incur excess losses due to the optical elements utilized to meet the design specifica-

[1] The article is published in the original.

tions. This elevates the complexity of the EDFA architecture in order to handle those losses.

This paper intends to investigate the performance of a variable gain-flattened L-band EDFA incorporating a DCM. Its ability to provide flat gain over L-band bandwidth spectrum was observed together with its maximum output power. The gains and noise figures under different input power and varying gains were studied. The effect of four-wave mixing (FWM) in the EDFA was also noted.

EDFA DESIGN CONCEPT

Table shows the specifications of the designed variable gain EDFA, which has an amplification bandwidth of 35 nm in the L-band window (1570 to 1605 nm). This bandwidth can support WDM transmission up to 44 channels at 100 GHz spacing. However, the power per channel is limited to 0 dBm in order to reduce the power injected into the DCM. The EDFA allows input signals ranging from –26 to 8 dBm and a maximum amplified output clamped at 23 dBm, which demonstrates adjustable gain range of 15 to 30 dB. The overall gain flatness is 1.5 dB with the best noise figure value of 5.2 dB expected to be achieved at operating gain of 30 dB. The noise figures are divided into 4 sections as seen in table, with the values worsening at lower operating gains.

The EDFA design is illustrated in Fig. 1, which shows 4 cascaded EDFA with the loss elements sandwiched in between the amplifiers. A DCM with 10 dB maximum loss was inserted in between EDFA 1 and 2. The amplified signals of EDFA 1 were set at 0 dBm per channel which brings the total combined output power to 16 dBm (40 channels, 100 GHz spacing). This is important in order to reduce any EDFA performance degradation due to the nonlinear effects brought upon by the small fiber core of the DCM. A variable optical attenuator (VOA) with maximum attenuation of 15 dB was placed after EDFA 2 to enable adjustments of the operating gain value. The maximum, attenuation of 15 dB was needed to allow gain variation of 15 to 30 dB as per the design objective. A gain equalizing filter (GEF) was the third loss element and was positioned prior to EDFA 4. The GEF was designed to have maximum insertion loss of 10 dB based on the total loss incurred by the passive components utilized in the EDFA as well as the intended maximum gain of 30 dB.

Specifications of variable gain-flattened EDFA

Parameter	Specification	Unit
Wavelength	1570–1605	nm
Input power dynamic range	–26–8	dBm
Gain adjustable range	15–30	dBm
NF for gain = 15 dB	13.5–14.0	dB
NF for gain = 20 dB	8.5–9.0	dB
NF for gain = 25 dB	6.2–6.5	dB
NF for gain = 30 dB	5.2–5.5	dB
Overall gain flatness	1.5	dB

AMPLIFIER ARCHITECTURE

Figure 2 shows the architecture of the variable gain EDFA studied in this work. Four 200 mW pump lasers at 1480 nm wavelength were used due to the high power conversion efficiency provided at that wavelength. The particular pump wavelength was also chosen based on the higher gain performance over 980 nm pumping, which was achieved by utilizing 1480 nm pumping with a bypass isolator [17]. Due to the limit on the signal power going into the DCM, the pump power for EDFA 1 was reduced in half with the remaining half routed to EDFA 3. One 1480 nm pump was used exclusively for EDFA 2 while the remaining 2 pump lasers provided bidirectional pumping for EDFA 4. During the experiment, all pump lasers are controlled via computer programming and the constant gain operation is performed by monitoring the signal condition at the input and output ports. Based

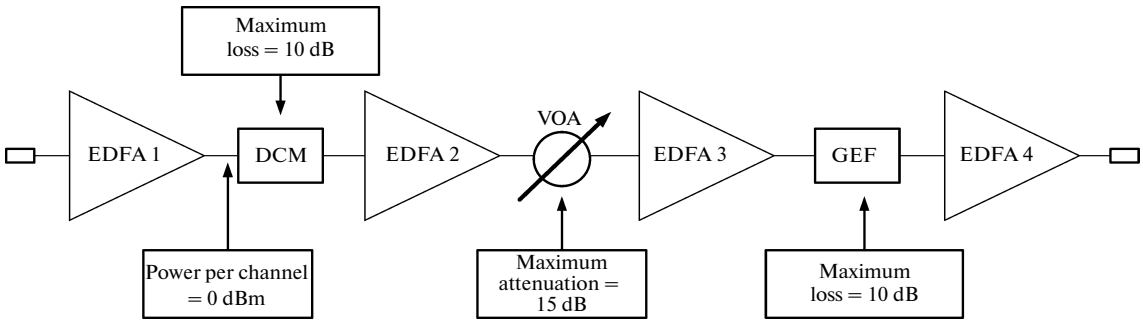

Fig. 1. Variable gain-flattened EDFA design concept.

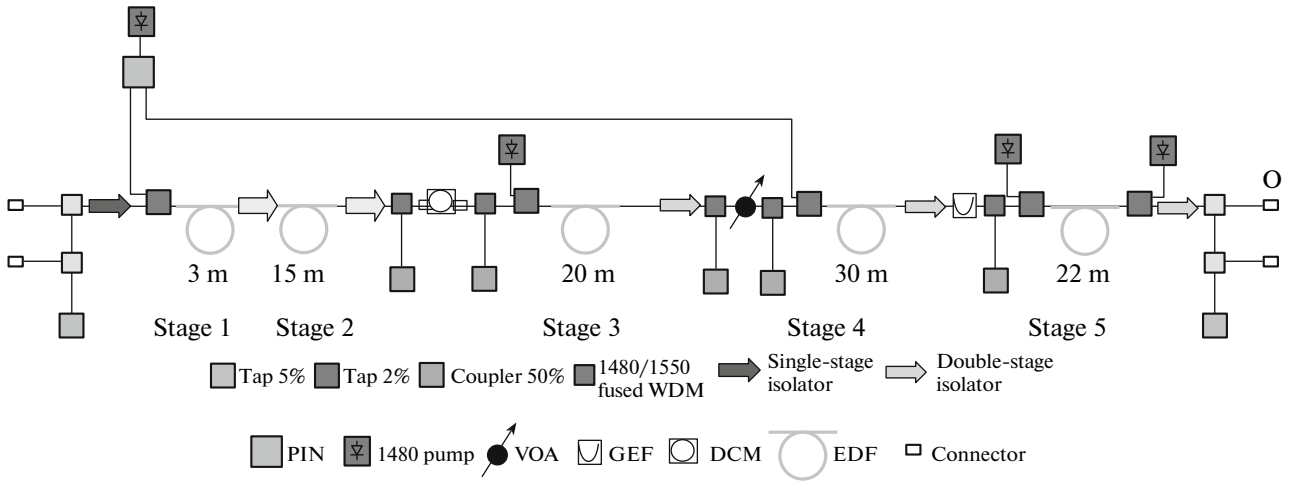

Fig. 2. Variable gain-flattened EDFA architecture.

on the gain control algorithm, all the operating conditions of pump lasers were automatically adjusted to keep the signal gain at the desired operating value.

The utilized erbium-doped fiber (EDF) has an absorption coefficient of 11 dB/m at 980 nm and 17.5 dB/m at 1531 nm with a numerical aperture of 0.22 dB and 900 nm cutoff wavelength. A total of 90 m of EDF was used in this architecture. EDFA 1 consisted of stage 1 and stage 2 with corresponding EDF lengths of 3 and 15 m separated by a double-stage isolator which has a high minimum isolation value. As Mahdi and Sheih reported, utilization of a bypass isolator enables the 1480 nm pump to pass through stage 1 to stage 2 with minimal insertion loss and the backward amplified spontaneous emission (ASE) can be significantly reduced [17]. The EDF lengths employed at stage 3, stage 4 and stage 5 are 20, 30, and 22 m, respectively. Since the length of EDF was significantly long to cater for L-band amplification, its sensitivity to temperature changes was also increased as article [18] reported, with gain and noise figure variations of up to 2.5 dB and 2.7 dB respectively as the temperature was adjusted from −10°C to 80°C. Therefore, in this experiment, all the fiber coils were heated at a constant temperature of 70°C to simulate the worst condition in practical field.

The technical challenges on producing GEF with high insertion loss value means that the maximum GEF loss for this work was constrained at 10 dB. The targeted GEF curve, which was obtained through simulation, exhibited maximum insertion loss of 7.2 dB as depicted in Fig. 3. Comparison was then made to the GEF curve measured from the fiber Bragg grating used as GEF in this experiment. It can be observed that the measured GEF curve shape complied with the simulated curve shape and the difference was only around ±0.3 dB. This gain error value indicates the minimum gain variation from 1570 to 1605 nm that can be achieved.

Overall, the spectra shown in Fig. 4 demonstrated excellent flatness of the multiple signal peaks under different operating gain. Less OSNR variations between signals were also expected since the ASE noise floor were quite uniform which can be attributed to the pumping arrangement of the amplifier. The exclusive pumping received by EDFA 2 enabled high output from stage 3 prior to the VOA. In turn, the signal coming from the VOA was of higher power thus allowing better utilization of the lower pumping power given to stage 4. More photons were then generated with the characteristic of the input signals thereby reducing the ASE noise going to the final EDFA stage. Nevertheless, a minor hump in the noise floor can be observed for 15 dB gain (Fig. 4a). This was caused by the higher attenuation required to obtain the gain, causing lower input signal coming from the VOA. The low input signal was unable to fully utilize the inverted erbium ions thus allowing higher ASE formation in that stage which was carried over to the next part. The

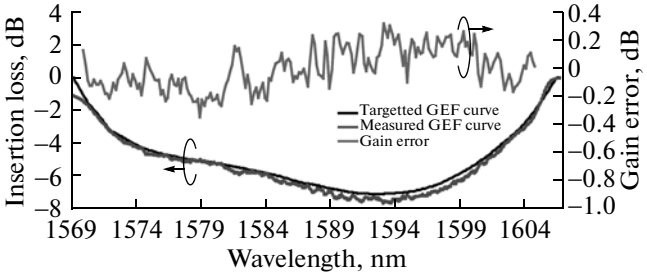

Fig. 3. Targeted and measured GEF curve.

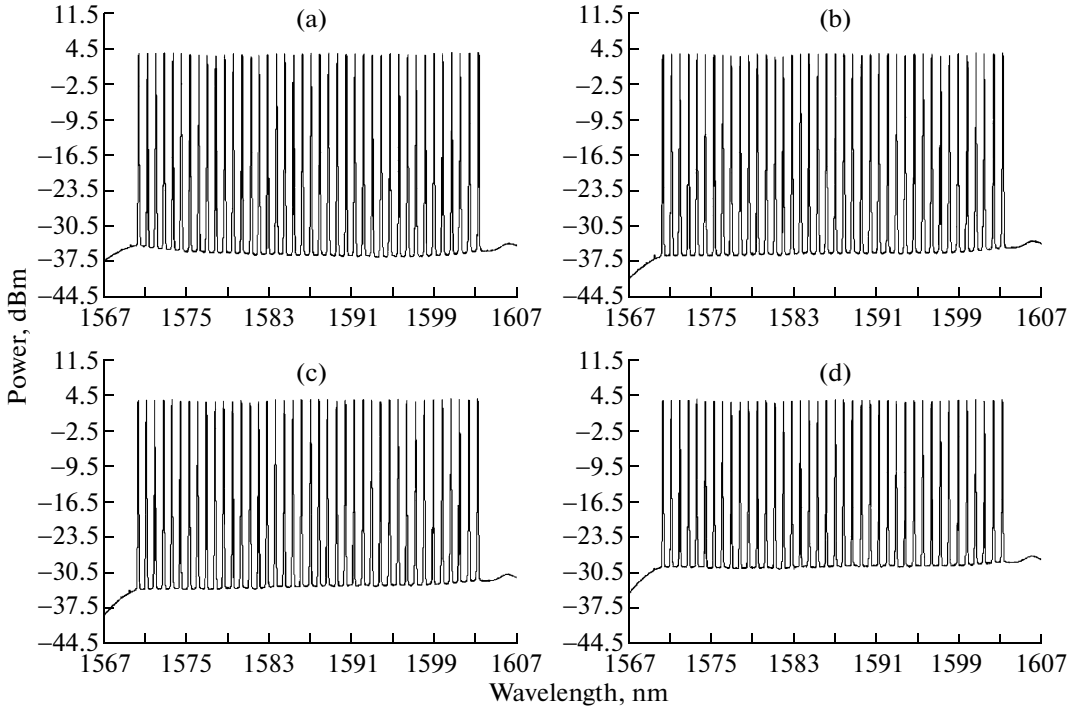

Fig. 4. Output spectrum at typical load of 40 channels at 8 dBm input signal and operating gain of (a) 15, (b) 20, (c) 25, and (d) 30 dB.

augmented ASE became dominant and acted as a broadband saturating tone which assisted in clamping the gain output [19]. There was less attenuation for the other operating gains which translated to higher signal level at VOA output. As a result, the ASE was reduced and from operating gain of 20 up to 30 dB, no ASE hump was detected. The same performance can also be obtained for input power of 7 dBm.

Figure 5 showcases the gain and noise figure values attained at different input signal power under varying operating gain value. The EDFA demonstrated excellent capability to provide the intended gain even at different input signal powers. The plotted gain graphs in Fig. 5a shows little disparity between each other and the shape of the graphs is generally similar for the various operating gains. The highest variations were observed at the gain of 15 and 20 dB where the variations reach 1 dB at input signals of 8 dBm and 3 dBm correspondingly. The best gain flatness was achieved at gain of 25 dB which has a gain variation of only 0.6 for −21 dBm input power. The average gain variation was only around 0.8 dB which is well below the specified gain flatness of 1.5 dB.

In Fig. 5b, discrepancies can be observed between the measured noise figures and the values specified in table at all operating gains, going as high as 2 dB at the longer wavelengths. The worst noise figures were noticed at gain of 15 dB where at the input signal of 8 dBm, the numbers were in excess of 14 dB while the noise figure for the lower power input of −11 dBm was lesser than 9 dB. For operating gain of 20 dB, the noise figure for input signal of −16 dBm was lower than the specified value of 8.5 dB but the opposite can be observed at 3 dBm input signal as the noise figure rose to more than 10 dB. The excessive noise figures was noted at the other operating gains as well, with the noise figure for −2 dBm input increasing to the 8 dB range for 25 dB gain while the 30 dB gain gave out noise figures higher than 6 dB at both high and low input signals. It can be discerned that higher input signals have worse noise figures compared to the low power inputs which can be attributed to the higher noise floor of the higher input signals which augmented the amount of broadband noise in the system. The use of multiple passive devices and lossy elements were also the contributing factors in this case. Additionally, the noise figures can be seen increasing at the longer wavelengths for the entire operating gain range, which can be explained by the noise equation for multi-stage amplifier [20],

$$F_{\text{multi–stage}} = F_1 + \frac{F_2 - 1}{G_1} + \frac{F_3 - 1}{G_1 G_2} + \ldots + \frac{F_n - 1}{G_1 G_2 \ldots G_{n-1}}. \quad (1)$$

As shown in Eq. (1), the dominant value in the total noise figure, $F_{\text{multi–stage}}$ is the noise figure of the first stage amplifier, F_1. The noise figures for subsequent stages, $F_{1, 2, 3 \ldots n}$ are dependent on the gains of the previous stages, $G_{1, 2 \ldots n-1}$ therefore reducing their impact

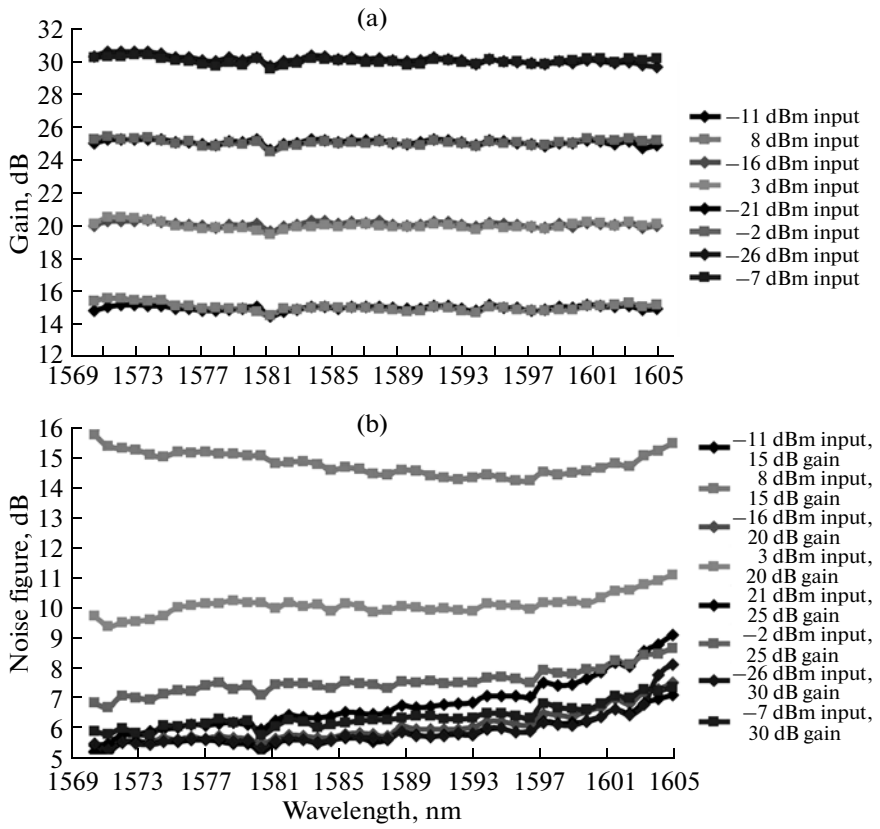

Fig. 5. Performance of the EDFA under different operating gains in terms of (a) gain and (b) noise figure.

on the total noise in the multi-stage EDFA. The noise figure for the EDFA 1 can be calculated using Eq. (2),

$$F = \left(1 + \frac{2P_{\text{ase}}}{h\nu B_0}\right)\frac{1}{G}. \quad (2)$$

Noise figure is calculated from several quantities such as P_{ase} which is the ASE power measured in bandwidth B_0. The rest are ν which is the optical frequency together with Planck's constant, h and the amplifier gain, G. From Eq. (2), it can be clearly observed that the EDFA noise figure is inversely proportional to the gain value. The fact that the emission rate of erbium is significantly lower at the longer wavelengths of L-band means that the gains in that particular region are substantially lower as well. Consequently, it affected the noise figures at the tail end of L-band window, causing them to increase significantly. This was further compounded by the fact that the gain of EDFA 1 was purposely limited to reduce nonlinear effects in DCM. The noise figures of the first EDFA was then carried over to the subsequent amplifiers, influencing the total noise figure of the multi-stage EDFA.

Optimizing the length of the first EDFA would allow for higher gains and lower noise figures at the far end of L-band. Nevertheless, this technique alone could not compensate for the effect of components losses that still persists. One method to counteract this problem is to separate the operating gain into two ranges, 15 to 22 dB gain for short transmission span and 23 to 30 dB gain for longer transmission distance. Since the higher gain range is not severely subjected to the high noise figures, it can continue to utilize the same EDFA specifications used in this work. On the other hand, the lower operating gain range will benefit from several adjustments to the EDFA architecture. Since the maximum gain for the lower range is only 22 dB, the length of the EDF employed in the stages can be significantly reduced therefore reducing fiber loss. The lower gain also means that the flat gain spectrum can be obtained from GEF with lower insertion loss. In addition, since the lower gain range amplifier is dedicated for short transmission span, this means that the accumulated dispersion would be lower as well thus the DCM length can be shortened. These steps would minimize the losses contributed by the lossy elements and consequently lessen the noise figure values.

Multiple channels in phase matching condition are susceptible to a phenomenon called four-wave mixing (FWM) [7]. In FWM, the energy of phase-matched signals is transferred to generate sidebands at different frequencies which will lessen the power of the original signals and induce in-band crosstalk. For conven-

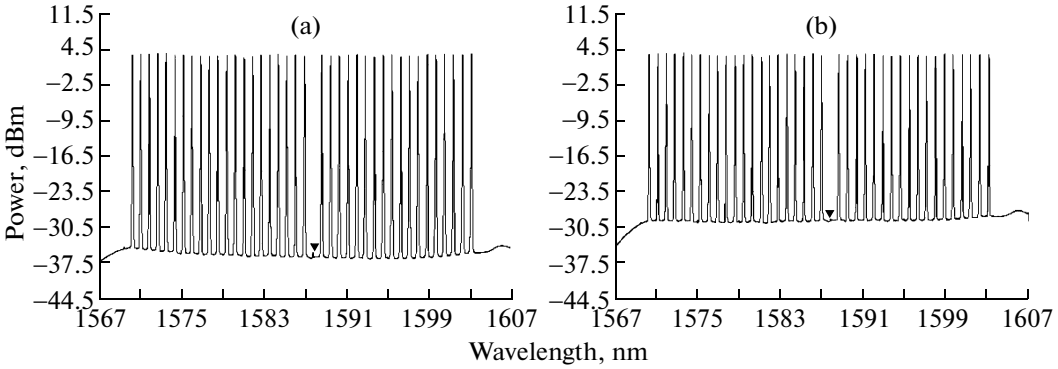

Fig. 6. Four-wave mixing viewed at operating gain of (a) 15 and (b) 30 dB.

tional transmission fiber, channels have to travel in phase matched condition for a considerable amount of distance before FWM can exist. In EDF, this phenomenon occurs in shorter length due to the higher nonlinearity of the fiber. Article [21] reported strong accumulation of FWM crosstalk in EDFA with increasing channel count.

The presence of FWM is depicted in Fig. 6, occurring at both minimum and maximum operating gain values of this EDFA. At operating gain of 15 dB, a 38 dB low value was measured while the worst value was a mere 32 dB low, which was experienced at the maximum gain. This value had little effect on the EDFA performance as the degradation of the Q parameter of the system was lesser than 1 [21]. The FWM decreased with lower output power since the power of the phase-matched original channels are reduced as well.

CONCLUSIONS

The design and development of a variable gain-flattened L-band EDFA was successfully accomplished. Four EDFA was cascaded and consisted of 5 stages with loss elements placed in between. The first EDFA was divided into two stages with a double-stage bypass isolator inserted in between to minimize the insertion loss between the stages while also assisting in reducing the backward ASE. The worse gain flatness observed was only at 0.6 dB over the 35 nm bandwidth and variable operating gain of 15 to 30 dB at varying input signal power of –26 to 8 dBm was successfully demonstrated. The output of the EDFA was also kept constant at 23 dBm at all gain values. Measured noise figure were substantially higher compared to the EDFA specifications due to the losses contributed by the passive and lossy components in the architecture along with the influence of the first stage amplifier noise figure. The elevated noise floor of the higher powered inputs was also responsible for the higher noise figure values of the larger input signals. This drawback can be countered by optimizing the length of the first stage amplifier to shift the gain spectrum towards the longer wavelength thus increasing the gain and reducing the noise figure at those particular points. Another way of reducing the noise figures is to separate the gain values into two, with the lower gain range benefiting from the use of lower loss components therefore lessening the noise figures.

ACKNOWLEDGMENTS

This work was partly supported by Universiti Putra Malaysia under Graduate Research Fellowship (GRF) scheme.

REFERENCES

1. Q. Wang and Q. X. Yu, Laser Phys. Lett. **6**, 607 (2009).
2. S. W. Harun, R. Parvizi, S. Shahi, and H. Ahmad, Laser Phys. Lett. **6**, 813 (2009).
3. C. H. Yeh, C. W. Chow, and C. L. Pan, Laser Phys. Lett. **8**, 130 (2011).
4. S. W, Harun, K. Dimyati, K. K. Jayapalan, and H. Ahmad, Laser Phys. Lett. **4**, 10 (2007).
5. H. Ahmad, N. K. Saat, and S. W. Harun, Laser Phys. Lett. **2**, 412 (2005).
6. S.-K. Liaw, C.-K. Huang, and Y.-L. Hsiao, Laser Phys. Lett. **5**, 543 (2008).
7. M. Jinno, T. Sakamoto, K. Jun-Ich, S. Aisawa, K. Oda, M. Fukui, H. Ono, M. Yamada, and K. Oguchi, IEEE. Photon. Technol. Lett. **10**, 454 (1998).
8. H. Ono, M. Yamada, M. Shimizu, and Y. Ohishi, Electron. Lett. **34**, 1513 (1998).
9. M. H. Abu Bakar, M. A. Mahdi, M. Mokhtar, A. F. Abas, and N. Md. Yusoff, Laser Phys. Lett. **6**, 602 (2009).
10. M. A. Mahdi, S. J. Sheih, and F. R. M. Adikan, Opt. Express **17**, 10069 (2009).
11. M. A. Mahdi, A. A. A. Bakar, M. H. Al-Mansoori, S. Shaari, and A. K. Zamzuri, Laser Phys. Lett. **5**, 126 (2008).

12. C. Yeh, T. Huang, M. Lin, C. Chow, and S. Chi, Laser Phys. **19**, 1246 (2009).
13. N. Md. Yusoff, M. H. Abu Bakar, S. J. Sheih, F. R. Mahamd Adikan, and M. A. Mahdi, Laser Phys. **20**, 1747 (2010).
14. A. R. Sarmani, S. J. Sheih, F. R. Mahamd Adikan, and M. A. Mahdi, Laser Phys. **20**, 1824 (2010).
15. P. F. Wysocki, J. B, Judkins, R. P. Espindola, M. Andrejco, and A. M. Vengsarkar, IEEE. Photon. Technol. Lett. **9**, 1343 (1997).
16. M. N. Islam, IEEE J. Sel. Top. Quant. **8**, 548 (2002).
17. M. A. Mahdi and S. J. Sheih, Opt. Commun. **237**, 295 (2004).
18. F. A. Flood, J. Lightwave Technol. **19**, 527 (2001).
19. M. A. Mahdi, S. Thirumeni, P. Poopalan, S. Selvakennedy, F. R. Mahamd Adikan, W. Y. Chan, and H. Ahmad, Opt. Fiber. Technol. **6**, 265 (2000).
20. M. A. Summerfield, J. Lightwave Technol. **18**, 1271 (2000).
21. Y. Liu, S. Burtsev, S. Tsuda, S. P. Hegarty, R. S. Mozdy, M. Hempstead, G. G. Luther, and R. G. Smart, Electron. Lett. **35**, 2130 (1999).